

# Anderson insulators as per Kohn's criterion: correlated, uncorrelated and deterministic disorder

Vipin Kerala Varma and Sebastiano Pilati

*The Abdus Salam International Centre for Theoretical Physics, Trieste, Italy*

(Dated: December 3, 2024)

The modern theory of the insulating state aims to describe all kinds of insulators within a unified theoretical formalism, independently of the physical mechanism which induces the insulating behaviour. Using this formalism, we investigate the metal-insulator transition in noninteracting disordered Fermi systems. We consider one-dimensional lattices with different types of aperiodic external potentials: uncorrelated disorder (one-dimensional Anderson model), deterministic disorder (Aubry-André model and its modification including next-nearest neighbour hopping), and disorder with long-range correlations (trace of fractional Brownian motion). We find that the many-body localisation tensor defined within the modern theory of the insulating state is a powerful probe to discriminate the insulating and the metallic phases and to locate the transition point in one-dimensional systems. In the three-dimensional Anderson model we find that the many-particle localisation tensor provides less sharp signals of the transition due to its deceptive system-size dependence in the dirty metal, calling for further investigations. Nevertheless we demonstrate that one can identify two regimes with conducting and insulating properties.

PACS numbers: 71.10.Fd, 71.30.+h, 71.23.An, 72.15.Rn

## I. INTRODUCTION

In the modern theory of the insulating state (MTIS), which was initiated by Kohn with the seminal article published in 1964, the different behaviour of metals and insulators are attributed to the different organisations of the electrons in the many-body ground state<sup>1</sup>. This approach is fundamentally different from the theory of band insulators, which attributes the insulating character to a gap in the excitation spectrum; or from the theory of Anderson localisation, which attributes it to the localised shape of the single-electron orbitals above the Fermi energy. Some fundamental developments in the MTIS were achieved only in the late 90's (thanks to the works by Resta and Sorella<sup>2</sup>, and others<sup>3,4</sup>) and led to a definition of the localisation tensor of a many-body system which is strongly connected to the Berry-phase estimator of the polarisation. This Berry-phase formalism permits one to compute the polarisation of extended systems and is nowadays routinely employed in the simulations of the electronic structure of solids<sup>5,6</sup>. The many-body localisation tensor can be derived also using a general geometric quantum theory<sup>7</sup>. It applies to any dimensionality and is related to experimentally measurable quantities, in particular to the polarizability and (for insulators<sup>8</sup>) conductivity sum-rules<sup>3</sup>. Furthermore, it is supposed to be adequate to describe any kind of insulator, independently from the physical mechanism which causes the insulating behaviour. Thus, it should apply to band, Mott<sup>2</sup>, Anderson<sup>9</sup>, quantum-Hall<sup>10</sup> and possibly even to topological insulators. Being natively designed for many-body systems, it represents a promising approach to investigate many-body localisation<sup>11,12</sup> in disordered interacting systems. So far, band and Mott insulators have been analysed in

the framework of the MTIS<sup>2</sup>, both using lattice models in a tight binding scheme, and also via ab-initio electronic structure simulations<sup>9,13-16</sup>. Instead, Anderson insulators have received little attention. In particular, it is not known whether the many-body localisation tensor can be used to distinguish conducting and insulating phases in noninteracting disordered systems, and to locate the critical point of this (Anderson) transition. The purpose of this article is to address this issue. With this aim, we study the Anderson transition in one-dimensional and in three-dimensional fermionic lattice models close to half filling. First, like Ref. 9, we consider one-dimensional lattices with uncorrelated disorder, where the single-electron orbitals are exponentially localised at any nonzero disorder strength. Then, we focus on the more intriguing and instructive case of deterministic disorder due to an external periodic potential, whose period is incommensurate with the lattice. It is known that all single-particle orbitals of this Hamiltonian (named Aubry-André model) become localised, but only beyond a finite disorder strength<sup>17</sup>. Thus, according to the Anderson criterion of localisation, a metal-insulator transition should occur at this disorder strength, for any lattice filling. Next, we consider a generalised Aubry-André model including next-nearest neighbour hopping. According to a recent study<sup>18</sup>, the single-electron orbitals of this Hamiltonian are localised if the corresponding energy is below a finite mobility edge, while they are extended otherwise, and the position of the mobility edge drifts with the disorder strength. The corresponding question is henceforth addressed in the many-particle context; that is, whether the MTIS predicts the phase-boundary between the metallic and the insulating phases to shift as the filling factor varies, consistently with the drift of the single-particle mobility edge. Further, the

case of non-deterministic disorder with tunable spatial correlations is also addressed. In particular, we consider a one-dimensional lattice where the on-site energies describe the trace of a (normalized) fractional Brownian motion. It has been shown that, in a certain regime, a finite portion of the single-particle spectrum hosts extended eigenstates, possibly leading to an insulator-to-metal transition in one dimension, in apparent contradiction with the one-parameter scaling theory of localisation<sup>19</sup>. Finally, we consider the three-dimensional Anderson model with uncorrelated disorder. This model represents the standard paradigm to explain the insulating transitions induced by disorder in bulk systems<sup>20,21</sup>. The corresponding single-particle spectrum hosts two mobility edges at weak disorder, whereas beyond a critical disorder strength, which has been accurately determined in several previous studies, all single-particle orbitals are localised.

This Article is organized as follows: in Section II we introduce the formalism of the MTIS, we provide the definition of the many-body localisation tensor and describe our numerical procedure to compute it. The analysis of the one-dimensional Anderson model is reported in Section III. The Aubry-André model is analysed in Section IV, and the generalised Aubry-André model in Section V. The one-dimensional Anderson model with long-range correlated disorder is studied in Section VI, and lastly the three-dimensional Anderson model in Section VII. In Section VIII we draw the conclusions, in particular we evaluate the effectiveness of the MTIS to identify insulating transitions in disordered systems, and we envision further developments.

## II. LOCALISATION TENSOR

Following Kohn's viewpoint on the origin of the insulating behaviour, the authors of Ref. 2 provided a quantitative definition of the many-body localisation tensor  $\lambda_{\alpha\beta}$  (the indices  $\alpha$  and  $\beta$  indicate spatial directions) which measures the degree of localisation of the particles in the many-body ground state and permits to discriminate metallic and insulating phases. In metals,  $\lambda_{\alpha\beta}$  is expected to be divergent in the thermodynamic limit, while it is finite in insulators, thus defining a many-body localisation criterion which is referred to as Kohn's localisation<sup>9</sup>.

The cases of periodic and open boundary conditions need to be treated separately because the position operator is ill defined in the former case<sup>22</sup>.

In the case of periodic boundary conditions the localisation tensor is obtained through the auxiliary quantity  $z_N^{(\alpha)}$ , which for a system of  $N$  particles is defined as<sup>2,7</sup>

$$z_N^{(\alpha)} = \langle \Psi | e^{i\frac{2\pi}{L}\hat{\mathbf{R}}_\alpha} | \Psi \rangle, \quad (1)$$

where  $|\Psi\rangle$  is the many-body ground state,  $\hat{\mathbf{R}}_\alpha$  is the  $\alpha$ -component of the many-body position operator  $\hat{\mathbf{R}} =$

$\sum_{i=1}^N \hat{r}_i$ , where  $\hat{r}_i$  is the single-particle position operator for particle  $i$ , with the index  $i = 1, \dots, N$ ;  $L$  is the linear system size. We consider spin-singlet ground states of spin-1/2 fermions, with  $N/2$  spin-up and  $N/2$  spin-down particles. For noninteracting particles,  $z_N^{(\alpha)}$  may be further simplified, obtaining<sup>7,23</sup>  $z_N^{(\alpha)} = \det^2 [S_{jj'}^{(\alpha)}]$ , where the matrix  $[S_{jj'}^{(\alpha)}]$  (with the indices  $j, j' = 1, 2, \dots, N/2$ ) is the overlap matrix whose elements are given by

$$S_{jj'}^{(\alpha)} = \int d\mathbf{r} \phi_j^*(\mathbf{r}) e^{i\frac{2\pi}{L}r_\alpha} \phi_{j'}(\mathbf{r}), \quad (2)$$

where  $\phi_j(\mathbf{r})$  are the single-particle eigenstate wavefunctions ordered for increasing energies, and  $\mathbf{r}$  is the spatial coordinate. Using this auxiliary quantity, the localisation tensor is now defined as<sup>2,23</sup>

$$\lambda_{\alpha\beta}^2 = -\frac{L^2}{4\pi^2 N} \log \frac{|z_N^{(\alpha)}| |z_N^{(\beta)}|}{|z_N^{(\alpha\beta)}|}, \quad (3)$$

where  $z_N^{(\alpha\beta)}$  is defined as in eq. (1) with  $R_\alpha$  replaced by  $R_\alpha - R_\beta$ . For half filling,  $N = L$  ( $N = L^3$ ) in one-dimension (in three-dimensions); from now on, without loss of generality, we consider the component of the localisation tensor corresponding to  $\alpha = \beta = x$ , which is given by  $\lambda_{xx}^2 = -L^{2-d} \log |z_N| / 2\pi^2$ , with  $d$  denoting dimensionality.

In the case of open boundaries, the position operator is well defined<sup>22</sup> and the localisation tensor may be evaluated according to the formula<sup>2,7</sup>

$$\lambda_{\alpha\beta}^2 = (\langle \psi_0 | \hat{\mathbf{R}}_\alpha \hat{\mathbf{R}}_\beta | \psi_0 \rangle - \langle \psi_0 | \hat{\mathbf{R}}_\alpha | \psi_0 \rangle \langle \psi_0 | \hat{\mathbf{R}}_\beta | \psi_0 \rangle) / N. \quad (4)$$

For a system of independent electrons with  $N/2$  spin-up and  $N/2$  spin-down particles, this may be further simplified to give the squared localisation length as<sup>7</sup>

$$\lambda_{\alpha\beta}^2 = \frac{1}{N} \int d\mathbf{r} d\mathbf{r}' (\mathbf{r} - \mathbf{r}')_\alpha (\mathbf{r} - \mathbf{r}')_\beta |\mathbf{P}(\mathbf{r}, \mathbf{r}')|^2, \quad (5)$$

where  $\rho(\mathbf{r}, \mathbf{r}') = 2P(\mathbf{r}, \mathbf{r}')$  is the one-particle density matrix for a Slater determinant, which is given by<sup>7</sup>

$$\rho(\mathbf{r}, \mathbf{r}') = 2 \sum_{j=1}^{N/2} \phi_j(\mathbf{r}) \phi_j^*(\mathbf{r}'). \quad (6)$$

We stress that the length-scale  $\lambda_{xx}$  is a many-body localisation length. In particular, it is not simply related to the spatial extent of the single-particle eigenstates. For example, in the case of noninteracting band insulators,  $\lambda_{xx}$  is related to the spread of the maximally localised Wannier functions<sup>3</sup>, rather than to the Bloch wave functions. Notice that the latter (which are the single-particle eigenstates) are always extended. There is no simple analogy with the Wannier functions for the case of disordered systems.

The formulation to compute the localisation length proposed in Refs. 2 and 7, and briefly summarized in this

section, provides a computational procedure to verify Kohn's contention that the many-body ground state contains sufficient information to ascertain whether the system is an insulator or a conductor, without recourse to the analysis of low-lying excitations. In this Article we provide evidence for a variety of disordered systems that this is indeed the case. The saturation of  $\lambda_{xx}^2$  in the thermodynamic limit is taken to signal Kohn's localisation<sup>2,9</sup>, whereas its divergence indicates a conductor.

In our computations we consider both periodic and open boundary conditions and employ, respectively, equations (3) and (5) to compute the localisation length. The single-particle wave-functions  $\phi_j(\mathbf{r})$ , needed to form the many-particle ground-state, are determined from exact diagonalisation of the Hamiltonian matrix for a single fermion using the Armadillo library<sup>24</sup>.

### III. 1D ANDERSON MODEL

We consider disordered tight-binding models of noninteracting spin-1/2 fermions defined by the Hamiltonian

$$H = t \sum_{r,\sigma} (b_{r,\sigma}^\dagger b_{r+1,\sigma} + \text{h.c.}) + W \sum_{r,\sigma} \epsilon_r n_{r,\sigma}, \quad (7)$$

where  $r = 1, \dots, L$  is the discrete index which labels the lattice sites,  $L$  is the linear system size,  $b_{r,\sigma}$  ( $b_{r,\sigma}^\dagger$ ) is the fermionic annihilation (creation) operator for a spin  $\sigma = \pm 1/2$  particle at site  $r$ , and  $n_{r,\sigma} = b_{r,\sigma}^\dagger b_{r,\sigma}$  is the corresponding particle number operator. Here and in the rest of the article the lattice spacing is used as the unit of length, and the (even) total number of fermions  $N$  is fixed. The hopping amplitudes to the nearest neighbours are set by  $t$ ,  $\epsilon_r$  is the (random) value of the energy at lattice site  $r$ , while the parameter  $W$  sets the strength of the disorder.

In this section we address, from a many-particle perspective, the Anderson model of localisation where the on-site energies  $\{\epsilon_r\}$  are sampled from a uniform probability distribution in the interval  $[-1, +1]$ . For noninteracting many-particle systems in the ground state, the wavefunction is obtained as the product of the Slater determinants (one per spin component) formed with the lowest-energy occupied single-particle orbitals. The number of fermions per spin component determines the Fermi energy. In this article, we consider the spin-singlet many-particle ground state of spin-1/2 fermions, having equal number of spin-up and spin-down particles. We recall that in one dimensional systems with uncorrelated disorder all single-particle orbitals are localised - meaning that they are characterised by an exponentially decaying envelope - for any nonzero disorder strength  $W$ . This follows from the one-parameter scaling theory, and precludes conductivity in the thermodynamic limit<sup>19</sup>. Since there is no mobility edge separating single-particle extended and localised states, according to the

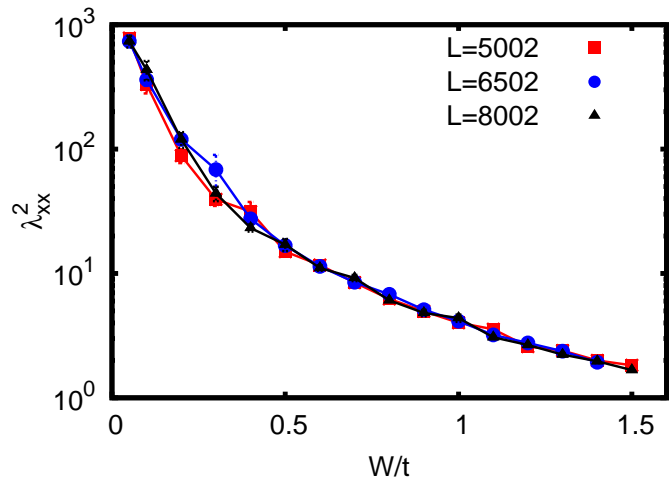


FIG. 1: (Colour online) Half-filled 1D Anderson model with periodic boundary conditions: Squared localisation length  $\lambda_{xx}^2$  (log-scale) as a function of the disorder strength  $W/t$ . Data for different systems sizes  $L$  are shown, and their mutual agreement indicates Kohn's localisation at all disorder strengths. The lines are guides to the eye. Here and in all figures the unit of length is the lattice spacing.

Anderson criterion of localisation the many-particle system should be an insulator at any filling.

In Fig. 1, we show the results for the squared localisation tensor  $\lambda_{xx}^2$  as a function of the disorder strength  $W/t$ . The data corresponding to three large (even) lattice sizes with periodic boundary conditions are shown. The lattices are half filled, and ensemble averaging of the results is performed considering 5–10 realisations of the disorder pattern. The localisation length  $\lambda_{xx}$  varies by a few orders of magnitude as we tune the disorder strength. However, it is always finite and system-size independent, in the whole range of disorder strengths we explore, which extends down to the extremely weak disorder  $W/t = 0.05$ . These findings constitute a clear signature of Kohn's localisation. Also, the variation of  $\lambda_{xx}^2$  with the disorder strength exhibits no sharp features (as opposed to the results of next sections). We verified that the data obtained using open boundary conditions (not shown) agree with those obtained using periodic boundary conditions.

Therefore, we conclude that the formalism of the MTIS predicts the many-particle ground-state of the 1D Anderson model to be an insulator, in agreement with the theory of Anderson localisation and the one-parameter scaling theory<sup>19</sup>. However, in this latter formalism the insulating character is attributed to the localised shape of the single-particle orbitals in the vicinity of the Fermi energy, while the MTIS immanently deals with the many-body ground-state wave-function.

#### IV. AUBRY-ANDRÉ MODEL

In this section we consider the one-dimensional Aubry-André model<sup>17</sup>. This is described by the Hamiltonian defined in eq. (7), but with the on-site energies given by the incommensurate potential  $\epsilon_r = \cos(2\pi r g)$ , where  $g = (\sqrt{5} + 1)/2$  is the golden ratio. This is an archetypal model to study Anderson transitions in lower dimensions; it has been experimentally realized with ultracold atomic gases trapped in bichromatic optical lattices<sup>25</sup>, and also in quasi-periodic photonic lattices<sup>26</sup>. The sinusoidal potential does not display periodicity on a finite lattice, and so the Aubry-André model is, in this

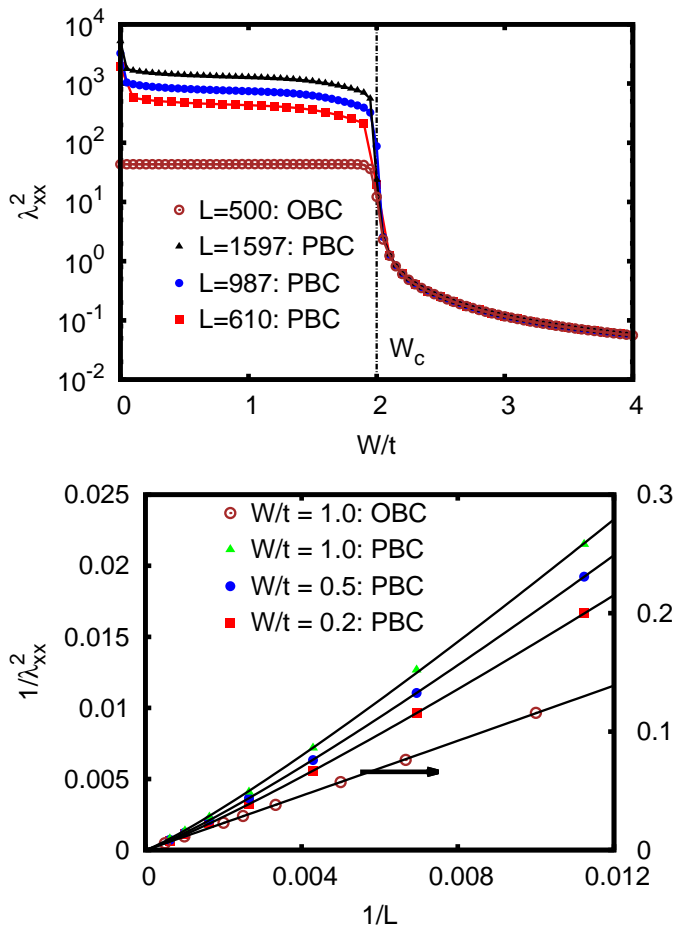


FIG. 2: (Colour online) Half-filled 1D Aubry-André model. Top panel: Squared localisation length  $\lambda_{xx}^2$  (log-scale) as a function of the quasi-disorder strength  $W/t$  for periodic (PBC) and open (OBC) boundary conditions, and for different Fibonacci lengths  $L$  of the chain; the vertical line indicates the critical disorder strength  $W_c/t = 2$ , separating extended from localised states. Bottom panel: Scaling of  $\lambda_{xx}^{-2}$  with the inverse system size  $1/L$  in the conducting phase  $W_c/t < 2$ . The continuous curves represent the power-law fits  $\lambda_{xx}^{-2} = cL^{-\gamma}$  ( $c$  and  $\gamma$  are fitting parameters).  $\lambda_{xx}^{-2}$  diverges with the exponent  $\gamma \approx 1.14$  for PBC (left axis) and with  $\gamma = 1.008(5)$  for OBC (right axis).

sense, disordered. However, this disorder is deterministic, and so is not truly random. In the presence of such “deterministic disorder”, as opposed to true disorder, the one-parameter scaling theory of Ref. 19 does not apply. In fact, it is known that this model hosts a transition from a diffusive phase at weak disorder, to a localised phase at strong disorder. In the former phase all single-particle eigenstates are extended over the whole system (possibly with the exception of a zero-measure set of non-exponentially localised states)<sup>17</sup>. In the latter phase they are all localised. The transition occurs at the critical disorder strength  $W_c/t = 2$ .

In simulations with periodic boundary conditions we need to consider system sizes given by Fibonacci numbers, so that the potential fits the periodicity of the lattice. The results for the squared localisation length  $\lambda_{xx}^2$  of half-filled lattices are displayed in Fig. 2 [top panel], both for periodic and open boundary conditions. A sharp variation of  $\lambda_{xx}^2$  occurs in the close vicinity of  $W/t = 2$ . For  $W/t > 2$ , the localisation length is finite and does not depend on the system size. This is a signature of Kohn’s localisation. Instead, for  $W/t < 2$ , a very rapid increase of  $\lambda_{xx}^2$  with the system size is observed, possibly indicating a metallic phase. In order to confirm this supposition we perform a detailed analysis of the finite-size scaling of  $\lambda_{xx}^2$ . Various datasets obtained in the regime  $W < 2$  are shown in Fig. 2 [bottom panel]. A best-fits analysis indicates that these data are accurately described by the (empirical) power-law fitting functions:  $\lambda_{xx}^{-2} = cL^{-\gamma}$ , where  $c$  and  $\gamma$  are the fitting parameters. The exponents obtained from the fitting procedure are  $\gamma = 1.135(2), 1.151(2), 1.14(1)$  (for  $W/t = 0.2, 0.5, 1$ ), and  $\gamma = 1.008(5)$  ( $W/t = 1$ ) for periodic and open boundary conditions, respectively. This fitting function predicts a divergence of the many-body localisation length in the thermodynamic limit, providing a clear indication of metallic behaviour. The divergence occurs both for periodic and open boundary conditions, but it is more rapid in the former case.

It is worth noticing that in the insulating phase the values of  $\lambda_{xx}^2$  obtained using periodic and open boundary conditions are indistinguishable within our numerical accuracy. This independence from the type of boundary conditions is indeed expected for insulators, since in these systems the localisation lengths (and the polarisation) are bulk properties, as opposed to metals where they depend on the size of the system.

The analysis of the Aubry-André model in the framework of the MTIS provides a clear signature of the metal-insulator transition at  $W/t = 2$ , in agreement with the Anderson criterion of localisation, which also predicts a phase transition at the same disorder strength since the single-particle orbitals change from extended to localised<sup>17</sup>. We point out that we also performed a similar analysis of the Aubry-André model at different lattice fillings in the regime  $0.1 < N/(2L) < 0.9$ , without observing measurable shifts of the critical point. This is also expected following Anderson’s criterion of localisa-

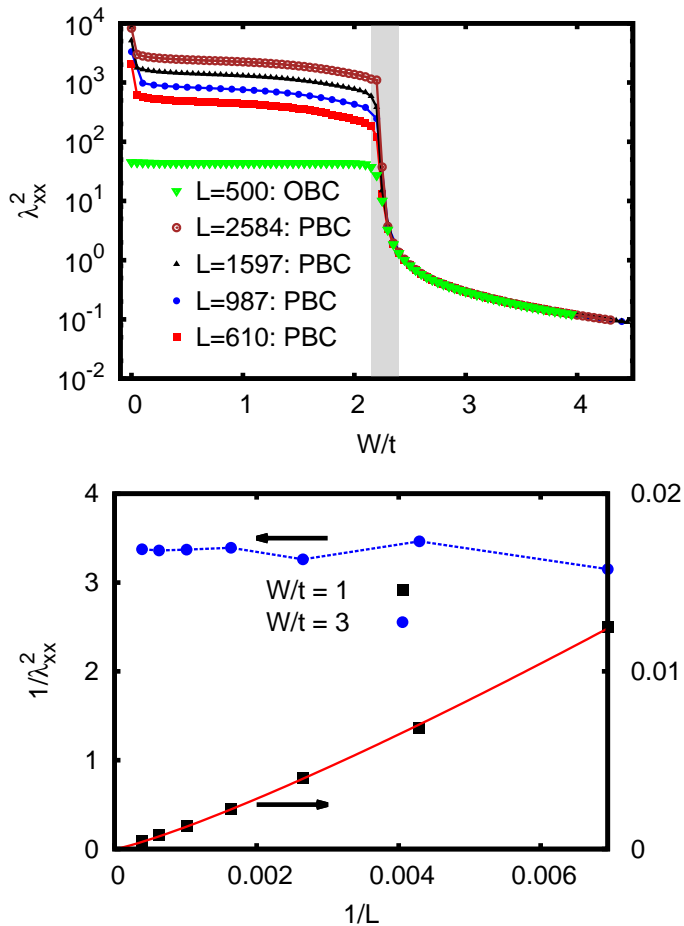


FIG. 3: (Colour online) Generalized 1D Aubry-André model with next-nearest hopping  $t_2/t = 0.5$ , at half filling. Top panel: Squared localisation length  $\lambda_{xx}^2$  (log-scale) as a function of the quasi-disorder strength  $W/t$ . Data for periodic (PBC) and open boundary conditions (OBC) are shown, for different chain lengths  $L$ . The gray vertical stripe indicates the approximate location of the critical point between the metallic and the insulating phases. Bottom panel: Scaling of inverse squared localisation length  $1/\lambda_{xx}^2$  with the inverse system size  $1/L$  at quasi-disorder strength in the metallic phase  $W/t = 1$  and in the insulating phase  $W/t = 3$  (blue dashed lines are a guide to eye). The continuous red curve represent the power-law fitting function  $\lambda_{xx}^2 = cL^{-\gamma}$ , with the best-fit parameter  $\gamma = 1.19(2)$ .

tion, since the single-particle spectrum of this model does not host mobility edges<sup>17</sup>.

## V. GENERALIZED AUBRY-ANDRÉ MODEL

Hopping processes beyond nearest-neighbour sites can dramatically alter the localisation properties, even causing the occurrence of single-particle mobility edges when none existed in the absence of such longer-range hoppings<sup>18</sup>. In this section, we consider the generalised

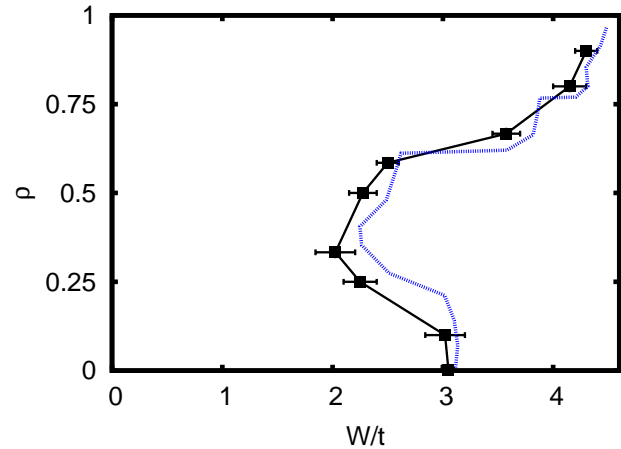


FIG. 4: (Colour online) Zero-temperature phase diagram of the generalised Aubry-André model with  $t_2/t = 0.5$ , as a function of filling  $\rho = N/(2L)$  and quasi-disorder strength  $W/t$ . The black points indicate the phase boundary separating the metallic phase (left) from the insulating phase (right) obtained within the MTIS. Our results may be compared with the critical point extracted from the inverse participation data of Ref. 18 (blue dashed curve).

Aubry-André model, including next-nearest neighbour hopping. With this modification, one obtains the Hamiltonian  $H' = H + t_2 \sum_{r,\sigma} (b_{r,\sigma}^\dagger b_{r+2,\sigma} + \text{h.c.})$ , where  $H$  is defined in eq. (7),  $t_2$  is the energy associated to hopping to next-nearest neighbours, and the on-site energies  $\epsilon_r$  are defined by the same incommensurate sinusoidal potential of the native Aubry-André model considered in the previous section.

This generalised Aubry-André model was studied in Ref. 18. The analysis of the single-particle spectrum based on calculations of the inverse participation ratio (which measures the spatial extent of the single-particle wave-functions) presented evidence of the presence of mobility edges in a certain regime of disorder strength  $W$ . The location of the mobility edges was found to vary with  $W$ . Like in previous sections, here we analyse the many-particle ground-state of the generalised Aubry-André Hamiltonian in the framework of the MTIS. We consider various lattice fillings, varying from vanishing density to full filling. We fix the next-nearest neighbour hopping at  $t_2/t = 0.5$ , a value which was also considered in Ref. 18. An illustrative example of the dependence of the squared localisation length  $\lambda_{xx}^2$  as a function of  $W$  is shown in Fig. 3 [top panel], where the datasets correspond to half-filled lattices of different sizes  $L$ . Here too, as in the case of the native Aubry-André model, a sharp variation of  $\lambda_{xx}$  occurs at a finite disorder strength  $W_c$ . For  $W > W_c$ ,  $\lambda_{xx}^2$  is finite and system-size independent, indicating Kohn's localisation. Instead, for  $W < W_c$ ,  $\lambda_{xx}^2$  rapidly increases as  $L$  increases. In order to assert whether in this regime the ground-state is metallic, we analyse the finite-size scaling of  $\lambda_{xx}^2$  (see Fig. 3 [bottom

panel]). The scaling of the squared localisation length with the system size  $L$  turns out to be accurately described by the empirical fitting function  $\lambda_{xx}^{-2} = cL^{-\gamma}$ , where  $c$  and  $\gamma$  are fitting parameters. At  $W/t = 1$ , the best fit is obtained with  $\gamma = 1.19(2)$ . This scaling behaviour clearly indicates a divergence of the localisation length, which is a signature of metallic behaviour.

In order to approximately pinpoint the phase boundary between the metal and the insulator, we determine the largest disorder strength where  $\lambda_{xx}$  clearly diverges in the thermodynamic limit, and the smallest value of  $W$  where it is system size independent, within numerical accuracy. This allows us to provide a (rather narrow) interval containing the critical disorder strength  $W_c$ . For the case of half-filling we obtain  $W_c/t = 2.275 \pm 0.125$ . This is displayed in Fig. 3 (see Fig. 3 [top panel]) as a gray vertical stripe.

By performing a similar analysis for different fillings, we obtain the zero-temperature phase diagram as a function of disorder strength and filling factor  $\rho = N/(2L)$  (see Fig. 4). The phase boundary separating the metallic and the insulating phases varies rapidly with the filling. Interestingly, these variations are non-monotonic: starting from the zero-density limit,  $W_c$  first decreases as the filling increases, then it rapidly increases when the filling is  $\rho \gtrsim 0.5$ .

These findings obtained within the MTIS can be compared with the prediction based on the Anderson criterion of localisation. We extract the location of the single-particle mobility edge from the contour plot data of the inverse participation ratio provided in Ref. 18. This procedure is based on the digitalisation of the colour-scale shown in Ref. 18, and so it entails some approximations. Vanishing values of the inverse participation ratio indicate extended single-particle orbitals, while finite values indicate localised states. The critical filling factor is obtained when the Fermi energy reaches the mobility edge. Notice that in Ref. 18 only the single lattice size  $L = 500$  was considered, without analysing the finite-size scaling behaviour. From the scattering of their data for  $L = 500$ , we estimate the indeterminacy on the extracted critical filling to be close to 10%. Therefore, performing a precise quantitative comparison between our data and those of Ref. 18 may not be completely justified. However, we see from Fig. 4 that the overall agreement is good. In particular, certain important feature of the ground-state phase diagram are predicted by both theories. First, in the low-filling limit both theories predict the critical disorder to be  $W_c/t \simeq 3$ , significantly larger than in the native Aubry-André model (where  $W_c/t = 2$ ). Second, the location of the phase boundary has large non-monotonic variations as a function of the filling factor.

## VI. 1D ANDERSON MODEL WITH CORRELATED DISORDER

The properties of the Anderson model defined in section III are affected in a non-trivial manner by the pres-

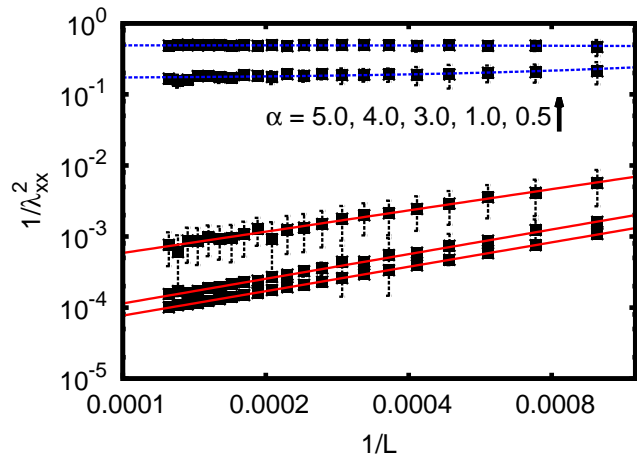


FIG. 5: (Colour online) Half-filled 1D Anderson model with long-range correlated disorder and PBC: Scaling of ensemble-averaged inverse squared localisation length  $1/\lambda_{xx}^2$  as a function of the inverse chain length  $1/L$  (log-log scale), for various values of the exponent  $\alpha$  characterising the disorder spectral density. For  $\alpha = 3.0, 4.0, 5.0$  our simulations indicate a divergence of  $\lambda_{xx}^2$  with system size, which is accurately described by the power-law fitting function  $\lambda_{xx}^{-2} = cL^{-\gamma}$  ( $c$  and  $\gamma$  are fitting parameters), shown as red solid lines. For  $\alpha = 0.5, 1$  the results suggest a saturation of  $\lambda_{xx}^2$  in the thermodynamic limit; the blue dotted lines indicate linear fits.

ence of spatial correlations in the disorder pattern, in particular if the correlations have a long-range character<sup>27–29</sup>. The effect of long-range spatial correlations has been investigated in several studies, considering in particular disorder patterns characterised by a power-law spectral density  $S(k) \propto k^{-\alpha}$ , where  $S(k)$  is the Fourier transform of the two-point correlation function  $\langle \epsilon_r \epsilon_{r'} \rangle$ , and the brackets  $\langle \dots \rangle$  indicate spatial averaging. The value of the exponent  $\alpha$  determines the extent of the spatial correlations. The case  $\alpha = 0$  corresponds to uncorrelated disorder. For  $\alpha > 2$  one has energy sequences with persistent increments<sup>29</sup>. A disorder pattern with power-law spectral density can be constructed using the following equation<sup>29</sup>:

$$\epsilon_r = \sum_{k=1}^{L/2} (k^{-\alpha} [2\pi/L]^{1-\alpha})^{1/2} \cos(2\pi r k/L + \phi_k), \quad (8)$$

where  $\phi_k$  (with  $k = 1, \dots, L/2$ ) are random phases sampled from a uniform distribution in the range  $[0, 2\pi]$ . This model is not designed for solid state systems. Instead, it is relevant to describe the electric transport in DNA molecules, and the trace of fractional Brownian motion<sup>29</sup>. In our calculations, we shift the on-site energies in order to obtain a disorder pattern with zero mean<sup>29</sup>:  $\epsilon_{\text{ave}} = \sum_r \epsilon_r = 0$ . Also, in order to curtail the growth of the disorder fluctuations as the system size increases, it is necessary to fix the magnitude of the variance of the on-site energies at  $\sum_r (\epsilon_r - \epsilon_{\text{ave}})^2 = 1$ , by appropriately rescaling the on-site energy distri-

bution<sup>29</sup>. Notice that, in the notation of eq. (7), the disorder-strength parameter is fixed at  $W/t = 1$ . This value is not equal to the maximum amplitude of the on-site random potential. This model of correlated disorder is non-deterministic, and so it differs in nature from the deterministic disorder of the Aubry-André models described in sections IV and V. However, its properties are also qualitatively different compared to the uncorrelated Anderson model of section III. In fact, a renormalisation group study<sup>29</sup> predicted that for large exponents  $\alpha > \alpha_c = 2$  the single-particle orbitals become extended in a finite portion of the energy spectrum close to the band centre. This is in sharp contrast with the case of uncorrelated disorder, where all single-particle orbitals are localised in one-dimensional systems<sup>19</sup>. It is worth emphasizing that the rescaling of the on-site energies was found to be crucial for the occurrence of the single-particle extended states<sup>30–32</sup>.

Fig. 5 reports the squared localisation length  $\lambda_{xx}^2$  in half-filled chains for various values of the exponent  $\alpha$ . The data points correspond to ensemble averages obtained using from 10 to 200 realisations of the disorder pattern. The error bars represent the standard deviation of the population (instead of the estimated standard deviation of the average) since, as pointed out in Ref. 33, in the presence of long-range correlations sample-to-sample fluctuations survive in the thermodynamic limit.

As seen from log-log scale of Fig. 5, the datasets corresponding to large exponents  $\alpha > \alpha_c$  display a clear power-law divergence of the localisation length  $\lambda_{xx}$  with the system size, indicating metallic behaviour in the many-particle system. Similarly to previous sections, we fit the disorder-averaged data for  $\alpha > 2$  with the fitting function  $\lambda_{xx}^{-2} = cL^{-\gamma}$ . The best fits are obtained with the exponents  $\gamma = 0.99(3), 1.15(1), 1.140(4)$ , for  $\alpha = 3.0, 4.0, 5.0$ , respectively. Notice that the latter two data are close to the values found for the Aubry-André model in the metallic phase. In contrast, for lower values of  $\alpha < 2$  the increase of  $\lambda$  with the system size saturates. This is confirmed by performing linear fits which extrapolate to finite values in the thermodynamic limit. These findings are consistent with the single-particle analysis of Ref. 29. Indeed, at half filling the Fermi energy is close to the band-centre, where the extended single-particle orbitals have been predicted to occur. Notice that, according to Ref. 33, ensemble-averaging causes the transition between single-particle localised and delocalised states to morph into a cross-over. However, our aim here is only to identify the two many-particle regimes with metallic and insulating phases, without focussing on the precise location of the transition point. In fact, we have checked that the two phases (with, respectively, diverging and saturating localisation lengths) can be unambiguously identified also by analysing the data corresponding to single realisations (not shown).

Our study, from the many-body perspective of the MTIS, substantiates the claim made in Ref. 29 vis-à-vis the oc-

currence of metallic states in 1D.

## VII. 3D ANDERSON MODEL

The three-dimensional Anderson Hamiltonian is a paradigmatic model used to describe the effect of disorder in bulk crystals<sup>20,21,34</sup>. It provides a setting where the electronic conductivity can be finite in the presence of uncorrelated disorder even in the thermodynamic limit<sup>19</sup>. In this section we report the first study of this model within the MTIS. The corresponding Hamiltonian, which is the extension to three dimensions of the model defined in section II with eq. (7), is given by

$$H = t \sum_{\mathbf{r}, \delta, \sigma} (b_{\mathbf{r}, \sigma}^\dagger b_{\mathbf{r} + \delta, \sigma} + \text{h.c.}) + W \sum_{\mathbf{r}, \sigma} \epsilon_{\mathbf{r}} n_{\mathbf{r}, \sigma}, \quad (9)$$

where the vector  $\mathbf{r} = (r_x, r_y, r_z)$  (with  $r_x, r_y, r_z = 1, \dots, L$ ) indicates the position on the lattice, and  $\delta = \{(1, 0, 0), (0, 1, 0), (0, 0, 1)\}$  connects nearest-neighbour lattice sites. Analogously to section II, we consider uncorrelated disorder generated by sampling the on-site energies  $\{\epsilon_{\mathbf{r}}\}$  from a uniform distribution in the interval  $[-1 : 1]$ . The single-particle spectrum of this model is characterised by the presence, at weak disorder, of two mobility edges (symmetric with respect to the band centre) separating localised from extended single-particle orbitals. At a critical disorder strength  $W_c$ , the two mobility edges collapse and all states become localised. Therefore, according to the Anderson criterion of localisation, at half-filling a metal to insulator transition occurs at  $W_c$ . In earlier works the mobility edges and  $W_c/t \simeq 8.25$  have been accurately determined using various computational techniques<sup>21,35–37</sup>, e.g. via transfer matrix theory and via analysis of level-spacing statistics.

Here we analyse the spin-singlet ground-state of the many-particle 3D Anderson model at half-filling within the MTIS. The results for the many-body localisation length in systems with both periodic and open boundary conditions are reported in Fig. 6 [left panel]. The datasets correspond to different lattice sizes, averaged over 5 – 100 disorder samples. The following three features of the results are noteworthy: (i) for strong disorder  $W \gg W_c$ ,  $\lambda_{xx}$  is essentially independent on the system size  $L$ , as expected for an insulating phase. (ii) for weaker disorder  $W \lesssim W_c$ ,  $\lambda_{xx}$  increases rapidly with the system size, as expected for a conducting phase. (iii) the difference between the localisation lengths computed with periodic and open boundaries (inset in Fig. 6, left panel) is negligible for strong disorder  $W \gg W_c$ , while it increases with the system size at weak disorder. This fact substantiates points (i) and (ii), since on general grounds one expects the choice of boundary conditions to be less important for insulators than for metals.

Despite these findings being consistent with the presence of a phase transition between a metallic and an insulating ground state, the available data do not allow us to quantitatively pinpoint the transition. We recall that in

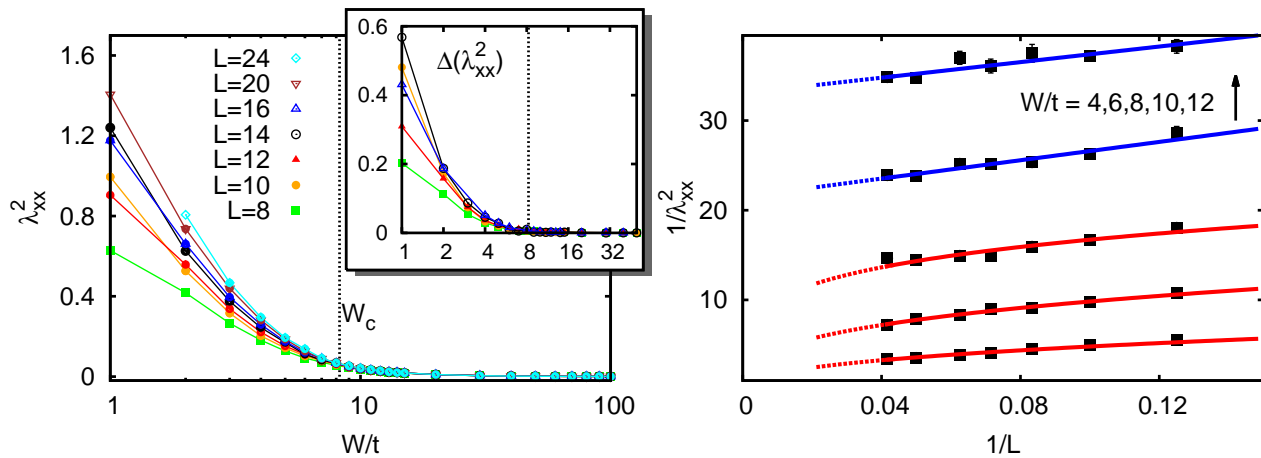


FIG. 6: (Colour online) Half-filled 3D Anderson model with uncorrelated disorder. Left panel: squared localisation length  $\lambda_{xx}^2$  as a function of disorder strength  $W/t$  (log-scale), for various system sizes  $L$ ; the vertical dashed line indicates the disorder strength  $W_c/t \simeq 8.25$  beyond which all single-particle orbitals are localised. The inset shows the difference  $\Delta(\lambda_{xx}^2) = \lambda_{xx,\text{PBC}}^2 - \lambda_{xx,\text{OBC}}^2$  between the squared localisation lengths obtained with periodic  $\lambda_{xx,\text{PBC}}^2$  and open boundary conditions  $\lambda_{xx,\text{OBC}}^2$ . Right panel: Scaling of the inverse squared localisation length with inverse system size  $1/L$ , for different disorder strengths  $W/t$ , increasing from bottom to top. The top two blue lines represent the linear fitting functions  $\lambda_{xx}^{-2} = a + b/L$  ( $a$  and  $b$  are fitting parameters) employed for  $W/t > 8$ . The lower three red curves represent power-law fitting functions  $\lambda_{xx}^{-2} = cL^{-\gamma}$  ( $c$  and  $\gamma$  are fitting parameters) employed for  $W/t < 8$ . The dashed portions of the curves represent the extrapolation towards the thermodynamic limit of the best-fits obtained from the relatively small systems sizes available.

order to identify a metallic phase within the MTIS, one should observe the divergence of the localisation length  $\lambda_{xx}$  with the system size<sup>2,7</sup>. The analysis of the finite-size scaling of  $\lambda_{xx}$  is shown in Fig. 6 [right panel]. At strong disorder, the data are accurately described by the linear fitting function  $\lambda_{xx}^{-2} = a + b/L$ , where  $a$  and  $b$  are the fitting parameters. The best fit is obtained with nonzero values of the infinite-size extrapolation  $a$ . This means that for sufficiently large lattices the signature of an insulating phase is recovered. At weak disorder  $W/t < 8.25$ , following the analyses performed in previous sections, we fit the data with the form  $\lambda_{xx}^{-2} = cL^{-\gamma}$ , where  $c$  and  $\gamma$  are fitting parameters. This fitting function, which predicts the divergence of the localisation length, accurately describes the data. For example, at  $W/t = 6$ , the reduced chi-squared is  $\chi^2/n_{\text{df}} = 1.22^2$ , where  $n_{\text{df}}$  is the number of degrees of freedom. However, we verified that the linear fitting function, which corresponds to insulating behaviour, would also fit the data with a finite value of  $a$  (e.g. at  $W/t = 6$ , we obtain  $\chi^2/n_{\text{df}} = 1.79^2$ ). This implies that the available data are insufficient to quantitatively determine the critical disorder strength  $W_c$  that separates the metallic and insulating phases. We attribute this deficiency to the small sizes which are feasible in three dimensions. Indeed, while in previous sections we obtained sharp indications of the metal-insulator transition using one-dimensional chains with linear sizes of order  $L \approx 10^3$ , in three-dimensions we can address linear sizes up to  $L = 24$ . This size is likely too small to identify the correct asymptotic scaling of  $\lambda_{xx}$  because the requirement<sup>7</sup>  $2\pi/L \approx 0$  is not quite satisfied. It should be emphasized here that the quantitative de-

termination of  $W_c$  is outside the scope of this article. We argue that a more refined theory on the scaling of the localisation length would be extremely beneficial for the application of the MTIS to three-dimensional systems. In particular, a theory predicting the values of the exponent  $\gamma$  or the linear coefficient  $b$  would make the fitting procedure more stringent. Insightful informations could be gained by investigating the long-distance behaviour of the one-body density matrix  $\rho(\mathbf{r}, \mathbf{r}')$  (see definition in (eq. 6)), as is evident from eq. (5), where the localisation length for open boundary conditions is determined as the second moment of the density matrix<sup>9</sup>. Therefore, the asymptotic behaviour of  $\rho(\mathbf{r}, \mathbf{r}')$  determines the system-size scaling of  $\lambda_{xx}^2$ . In fact, it is known that in clean metals  $\rho(\mathbf{r}, \mathbf{r}')$  has an asymptotic algebraic decay<sup>38</sup>, as opposed to gapped insulators where this decay is exponential<sup>39-41</sup>, with a polynomial pre-factor in one-dimension<sup>42</sup>. To the best of our knowledge, no precise information is available for dirty metals, calling for further investigations.

## VIII. CONCLUSIONS

We have investigated the Anderson transitions in noninteracting fermionic lattice models close to half filling within the modern theory of the insulating state. Our findings present evidence that the many-body localisation tensor introduced in Ref. 2 provides a clear signature of the insulating transition induced by disorder at zero temperature. This was verified in one-dimensional models with uncorrelated disorder,

deterministic disorder due to incommensurate potentials, and disorder with long-range correlations described by a power-law spectral function. In particular, it was verified that the ground-state of the one-dimensional Anderson model is insulating at any disorder strength, in agreement with the one-parameter scaling theory<sup>19</sup> of Anderson localisation. In the cases of deterministic and correlated disorder, we found evidence of metal-insulator transitions, in agreement with previous studies on the critical disorder strength and on the position of the mobility edge based on single-particle theories. Our results for the 3D Anderson model are more subtle. By using the tools of the MTIS we obtained evidence of two regimes with, respectively, metallic and insulating properties, as inferred from the sensitivity of the many-body localisation length to system size and boundary conditions. However, it was not possible to quantitatively locate the critical point. This limitation could be resolved by a better understanding of the finite-size scaling of the many-body localisation tensor and of the long-distance dependence of the one-body density matrix in dirty metals.

We emphasize that the MTIS allows us to address the Anderson transition from a many-body perspective.

Indeed in previous studies the MTIS has been successfully applied to the Mott transition in (clean) correlated electronic systems<sup>2,13,16</sup>. Thus our work paves the way to future investigations on the fate of the Anderson localisation in the presence of interactions<sup>11</sup> within the formalism of the MTIS. Such studies would shed light on the potential intriguing connection between Kohn's criterion for the metal-insulator transition, which is based on a measure of localization in the many-particle configuration space<sup>1,2,7</sup>, and the many-body localisation defined in more recent works<sup>12,43</sup>, which is associated to localisation in Fock space and to the breakdown of thermalization. One appealing technical feature of the MTIS is that it permits to identify the insulating phase using only ground-state properties, differently from other techniques employed for identifying metal-insulator transitions (particularly in disordered systems), which require information about excited states. This feature makes it suitable for large scale computational approaches like quantum Monte Carlo simulations<sup>15,16</sup>.

We acknowledge insightful comments from R. Resta on the manuscript, help from M. Atambo with computing facilities, and interesting discussions with J. Goold.

- 
- <sup>1</sup> W. Kohn, Phys. Rev. **133**, A171 (1963).  
<sup>2</sup> R. Resta and S. Sorella, Phys. Rev. Lett. **82**, 370 (1999).  
<sup>3</sup> I. Souza, T. Wilkins, and R. M. Martin, Phys. Rev. B **62**, 1666 (2000).  
<sup>4</sup> N. Marzari and D. Vanderbilt, Phys. Rev. B **56**, 12847 (1997).  
<sup>5</sup> R. Resta and D. Vanderbilt, in *Physics of Ferroelectrics* (Springer Berlin Heidelberg, 2007), vol. 105 of *Topics in Applied Physics*, pp. 31–68.  
<sup>6</sup> N. A. Spaldin, J. Solid State Chem. **195**, 2 (2012).  
<sup>7</sup> R. Resta, Eur. Phys. J. B **79**, 121 (2011).  
<sup>8</sup> R. Resta, private communication.  
<sup>9</sup> G. L. Bendazzoli, S. Evangelisti, A. Monari, and R. Resta, J. Chem. Phys. **133**, 064703 (2010).  
<sup>10</sup> R. Resta, Phys. Rev. Lett. **95**, 196805 (2005).  
<sup>11</sup> L. Fleishman and P. W. Anderson, Phys. Rev. B **21**, 2366 (1980).  
<sup>12</sup> D. M. Basko, I. L. Aleiner, and B. L. Altshuler, Ann. Phys. **321**, 1126 (2006).  
<sup>13</sup> V. Vetere, A. Monari, G. L. Bendazzoli, S. Evangelisti, and B. Paulus, J. Chem. Phys. **128**, 024701 (2008).  
<sup>14</sup> M. Veithen, X. Gonze, and P. Ghosez, Phys. Rev. B **66**, 235113 (2002).  
<sup>15</sup> N. D. M. Hine and W. M. C. Foulkes, J. Phys. Condens. Matter **19**, 506212 (2007).  
<sup>16</sup> L. Stella, C. Attacalite, S. Sorella, and A. Rubio, Phys. Rev. B **84**, 245117 (2011).  
<sup>17</sup> S. Aubry and G. André, Ann. Isr. Phys. Soc. **3**, 133 (1980).  
<sup>18</sup> J. B. Jr., D. J. Priour, B. Wang, and S. D. Sarma, Phys. Rev. B **83**, 075105 (2001).  
<sup>19</sup> E. Abrahams, P. W. Anderson, D. C. Licciardello, and T. V. Ramakrishnan, Phys. Rev. Lett. **42**, 673 (1979).  
<sup>20</sup> P. W. Anderson, Phys. Rev. **109**, 1492 (1958).  
<sup>21</sup> B. Kramer and A. MacKinnon, Rep. Prog. Phys. **56**, 1469 (1993).  
<sup>22</sup> R. Resta, Phys. Rev. Lett. **80**, 1800 (1998).  
<sup>23</sup> R. Resta, J. Phys.: Condens. Matter **14**, R625 (2002).  
<sup>24</sup> C. Sanderson, Technical Report NICTA (2010).  
<sup>25</sup> G. Roati, C. D'Errico, L. Fallani, M. Fattori, C. Fort, M. Zaccanti, G. Modugno, M. Modugno, and M. Inguscio, Nature **453**, 895 (2008).  
<sup>26</sup> Y. Lahini, R. Pugatch, F. Pozzi, M. Sorel, R. Morandotti, N. Davidson, and Y. Silberberg, Phys. Rev. Lett. **103**, 013901 (2009).  
<sup>27</sup> M. J. V. C. M. Soukoulis and E. N. Economou, Phys. Rev. B **50**, 5110 (1994).  
<sup>28</sup> F. M. Izrailev and A. A. Krokhin, Phys. Rev. Lett. **82**, 4062 (1999).  
<sup>29</sup> F. de Moura and M. L. Lyra, Phys. Rev. Lett. **81**, 3735 (1998).  
<sup>30</sup> J. W. Kantelhardt, S. Russ, A. Bunde, S. Havlin, and I. Webman, Phys. Rev. Lett. **84**, 198 (2000).  
<sup>31</sup> F. A. B. F. de Moura and M. L. Lyra, Phys. Rev. Lett. **84**, 199 (2000).  
<sup>32</sup> S. Russ, J. W. Kantelhardt, A. Bunde, and S. Havlin, Phys. Rev. B **64**, 134209 (2001).  
<sup>33</sup> S. Nishino, K. Yakubo, and H. Shima, Phys. Rev. B **79**, 033105 (2009).  
<sup>34</sup> E. Abrahams, *50 years of Anderson Localization* (World Scientific, 2010).  
<sup>35</sup> E. Hofstetter and M. Schreiber, Phys. Rev. B **49**, 14726 (1994).  
<sup>36</sup> K. Slevin and T. Ohtsuki, Phys. Rev. Lett. **82**, 382 (1999).  
<sup>37</sup> A. Rodriguez, L. J. Vasquez, K. Slevin, and R. A. Römer, Phys. Rev. B **84**, 134209 (2011).  
<sup>38</sup> S. Ismail-Beigi and T. A. Arias, Phys. Rev. Lett. **82**, 2127

- (1999).
- <sup>39</sup> W. Kohn, Phys. Rev. **115**, 809 (1959).
- <sup>40</sup> J. D. Cloizeaux, Phys. Rev. **135**, 698 (1964).
- <sup>41</sup> S. N. Taraskin, D. A. Drabold, and S. R. Elliott, Phys. Rev. Lett. **88**, 196405 (2002).
- <sup>42</sup> L. He and D. Vanderbilt, Phys. Rev. Lett. **86**, 5341 (2001).
- <sup>43</sup> V. Oganesyan and D. A. Huse, Phys. Rev. B **75**, 155111 (2007).